Charged lepton flavour violation
Overview of current experimental limits and future plans

Ann-Kathrin Perrevoort[a],∗ on behalf of the Mu3e Collaboration

[a]*Institute of Experimental Particle Physics, Karlsruhe Institute of Technology,*
Hermann-von-Helmholtz-Platz 1, Eggenstein-Leopoldshafen, Germany

E-mail: ann-kathrin.perrevoort@kit.edu

The observation of lepton flavour violation in the charged lepton sector (cLFV) would be an unambiguous sign of physics beyond the Standard Model of particle physics. cLFV processes are investigated in a multitude of channels at various experiments but have eluded observation so far. In the following, a selection of recent results as well as prospects on cLFV in heavy di-lepton resonances, Higgs, Z, B, kaon, τ and muon decays is presented.

∗Speaker

1. Charged lepton flavour violation

In its original formulation, the Standard Model of particle physics (SM) conserves lepton flavour although this conservation only arises from an accidental symmetry. Indeed, the observation of neutrino oscillations has proven that lepton flavour is violated in nature – at least in the neutral lepton sector. Simply extending the SM to account for neutrino masses and mixing, though, yields negligible amounts of LFV in processes involving charged leptons. The process $\mu \to e\gamma$, for example, is suppressed to branching ratios below 10^{-54} and thus far below what could be observed in experiments. Numerous models beyond the SM (BSM), however, predict increased and potentially observable rates of charged LFV (cLFV) (see e.g. [1] for an overview). This turns cLFV searches into powerful probes of BSM physics.

Despite numerous searches in a variety of channels, cLFV has eluded observation so far. These searches range from cLFV in Higgs and Z boson decays at general-purpose experiments to muon-to-electron transitions at specialised experiments. The derived upper exclusion limits on the branching ratio $\mathscr{B}$ of cLFV processes span ten orders of magnitude, from 10^{-3} in Higgs decays down to 10^{-13} in muon decays with prospects to reach sensitivities to $\mathscr{B}$ of around 10^{-17} in the coming years. A selection of searches is presented in the following.

2. General-purpose experiments

Collider experiments enable cLFV searches at the highest available energies. The current most stringent limits in this regime are held by the ATLAS and CMS experiments at the Large Hadron Collider (LHC) at CERN.

CMS has performed a search for heavy di-lepton ($\ell\ell'$) resonances with the full Run 2 data set of $138\,\mathrm{fb}^{-1}$ of pp collisions at a centre-of-mass energy $\sqrt{s}$ of 13 TeV [2]. Such a resonance can occur for example from τ-sneutrinos $\tilde{\nu}_\tau$ in R parity violating, super-symmetric models (RPV-SUSY), LFV Z' and quantum black holes (QBH). The resonance would emerge as an excess on top of the reconstructed mass spectra of the $\ell\ell'$ final state. Backgrounds stem from top decays, di-boson events, leptonic decays of Z bosons as well as mis-identified leptons. In the case of an $e^\pm\mu^\mp$ final state, the invariant mass ($m_{e\mu}$) spectrum is studied. In the case of an $e^\pm\tau^\mp$ or $\mu^\pm\tau^\mp$ resonance, hadronically decaying τ-leptons (τ_{had}) are considered in the analysis and the search is performed on the collinear mass spectrum. The mass spectra are shown in Fig. 1.
No statistically significant excess of data above the expected background has been found. Limits on the masses of LFV $\tilde{\nu}_\tau$, Z' and quantum black holes in benchmark models are set in the TeV range. A summary is given in Table 1. Model-independent limits are shown in Fig. 1.

In addition to heavy $\ell\ell'$ resonances, LFV decays of Higgs and Z bosons are searched for at the ATLAS and CMS experiments. Similarly to the heavy $\ell\ell'$ resonance searches, LFV searches of H and Z to an $e\mu$ final state are performed as searches for an excess in the invariant $m_{e\mu}$ mass spectra (see Fig. 2a). In an analysis of the full Run 2 data set of $139\,\mathrm{fb}^{-1}$ of pp collisions at $\sqrt{s}$ = 13 TeV, ATLAS has excluded $H \to e^\pm\mu^\mp$ at branching ratios above 6.2×10^{-5} at 95 % CL [3], and $Z \to e^\pm\mu^\mp$ above 2.62×10^{-7} at 95 % CL [4]. CMS sets an even stronger upper exclusion limit on $\mathscr{B}(H \to e^\pm\mu^\mp)$ at 4.4×10^{-5} at 95 % CL in a full Run 2 analysis by deploying a boosted decision tree for improved signal-to-background discrimination [5].
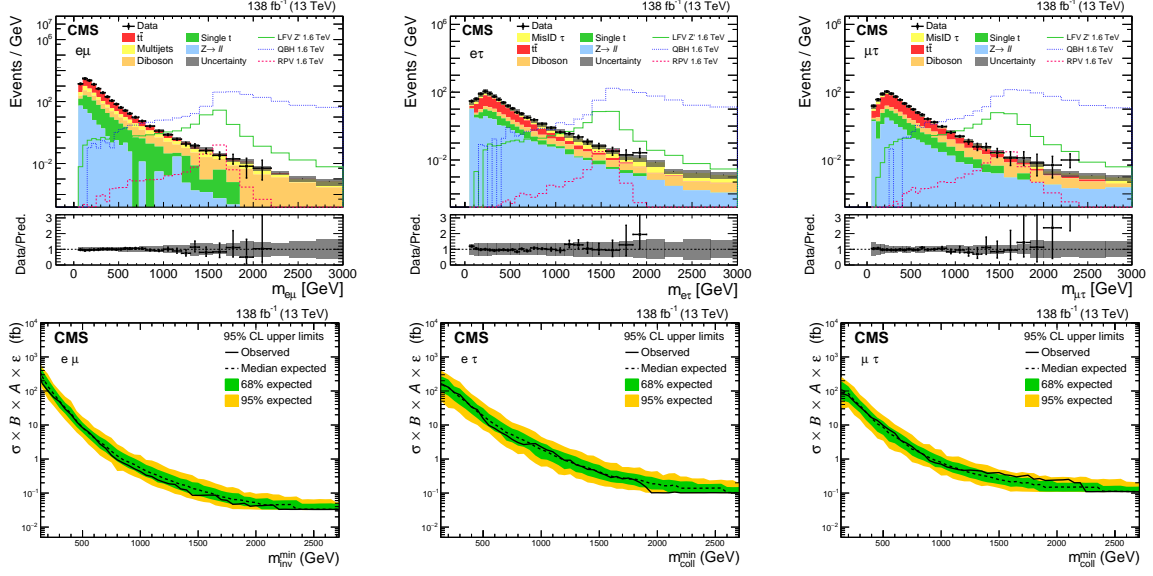
2

Figure 1: Invariant mass distributions (top) and model-independent upper limits on the product of the cross-section, branching ratio, acceptance and efficiency at 95 % CL (bottom) of the $e\mu$ (left), $e\tau$ (centre) and $\mu\tau$ (right) channel of the search for heavy $\ell\ell'$ resonances [2].

| | RPV-SUSY $\tilde{\nu}_\tau$ [TeV] | | LFV Z' [TeV] | QBH m_{th} [TeV] |
	$\lambda = \lambda' = 0.01$	$\lambda = \lambda' = 0.1$	$\mathcal{B} = 0.1$	$n = 4$
$e\mu$	2.2 (2.2)	4.2 (4.2)	5.0 (4.9)	5.6 (5.6)
$e\tau_{\text{had}}$	1.6 (1.6)	3.7 (3.7)	4.3 (4.3)	5.2 (5.2)
$\mu\tau_{\text{had}}$	1.6 (1.6)	3.6 (3.7)	4.1 (4.2)	5.0 (5.0)

Table 1: Observed (expected) upper limits at 95 % CL on the masses of RPV-SUSY sneutrinos, LFV Z' and quantum black holes (QBH) in benchmark models [2].

In $H \to \ell\tau$ and $Z \to \ell\tau$ searches with the full Run 2 data set at the ATLAS and CMS experiments, both hadronically and leptonically decaying τ leptons are reconstructed. In the latter case, only events with an $e^\pm\mu^\mp$ final state are considered to avoid large background contributions from SM $Z \to \ell\ell$ and $H \to \ell\ell$ decays. The analyses deploy either a boosted decision tree ($H \to \ell\tau$) or a neural network ($Z \to \ell\tau$) for signal and background discrimination (see Fig. 2b and 2c).
CMS has set upper exclusion limits of $\mathcal{B}(H \to e^\pm\tau^\mp) < 0.22\,\%$ and $\mathcal{B}(H \to \mu^\pm\tau^\mp) < 0.15\,\%$ at 95 % CL [6]. ATLAS reaches comparable exclusion limits with $\mathcal{B}(H \to e^\pm\tau^\mp) < 0.20\,\%$ and $\mathcal{B}(H \to \mu^\pm\tau^\mp) < 0.18\,\%$ at 95 % CL [7]. Exclusion limits on cLFV Higgs Yukawa couplings are shown in Fig. 3. In the case of $Z \to \ell\tau$, ATLAS holds the currently most stringent limits with $\mathcal{B}(Z \to e^\pm\tau^\mp) < 5.0 \times 10^{-6}$ and $\mathcal{B}(Z \to \mu^\pm\tau^\mp) < 6.5 \times 10^{-6}$ at 95 % CL [8, 9].

LFV processes can also occur in the production and decay of top quarks. CMS has performed a search for $q \to e\mu t$ production and $t \to e\mu q$ decay with $q = u, c$ on the full Run 2 data set [10]. Events with an $e^\pm\mu^\mp$ pair and at least one b jet are selected. The backgrounds, dominantly from events with $t\bar{t}$ and tW pairs, are suppressed with a boosted decision tree. The signal is parameterised
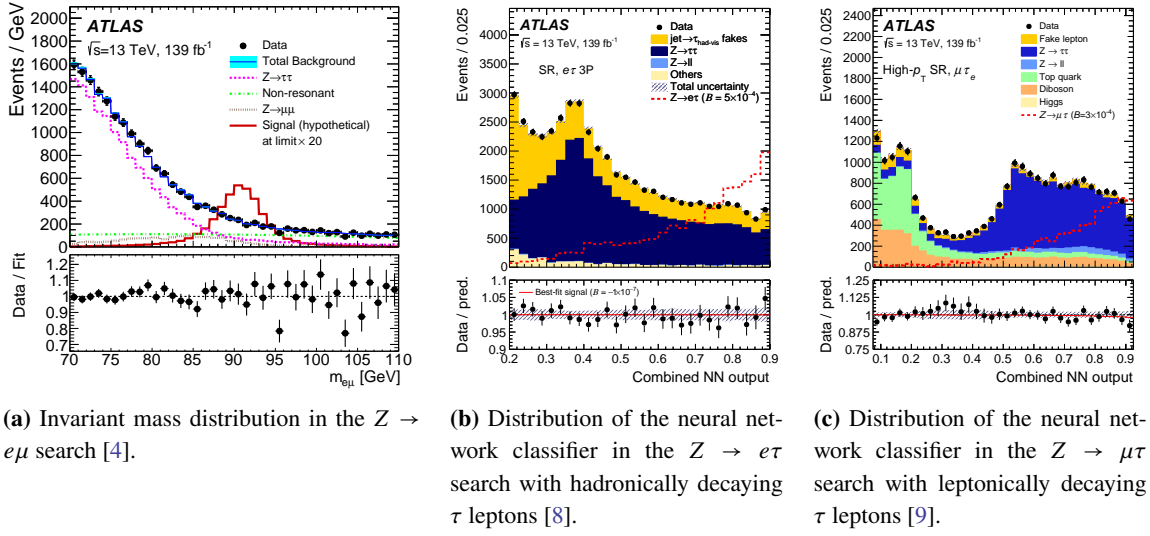
(a) Invariant mass distribution in the $Z \to e\mu$ search [4].

(b) Distribution of the neural network classifier in the $Z \to e\tau$ search with hadronically decaying τ leptons [8].

(c) Distribution of the neural network classifier in the $Z \to \mu\tau$ search with leptonically decaying τ leptons [9].

Figure 2: Distributions of the invariant mass and neural network classifier in $Z \to \ell\ell'$ searches, respectively [4, 8, 9].
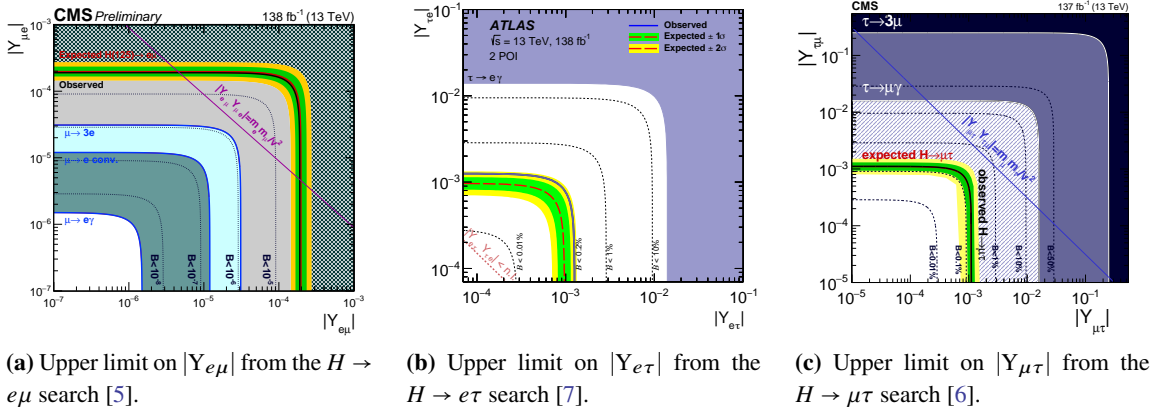

(a) Upper limit on $|Y_{e\mu}|$ from the $H \to e\mu$ search [5].

(b) Upper limit on $|Y_{e\tau}|$ from the $H \to e\tau$ search [7].

(c) Upper limit on $|Y_{\mu\tau}|$ from the $H \to \mu\tau$ search [6].

Figure 3: Upper limits on the cLFV Higgs Yukawa couplings $|Y_{\ell\ell'}|$ at 95 % CL derived in the searches for $H \to \ell\ell'$ decays [5–7].
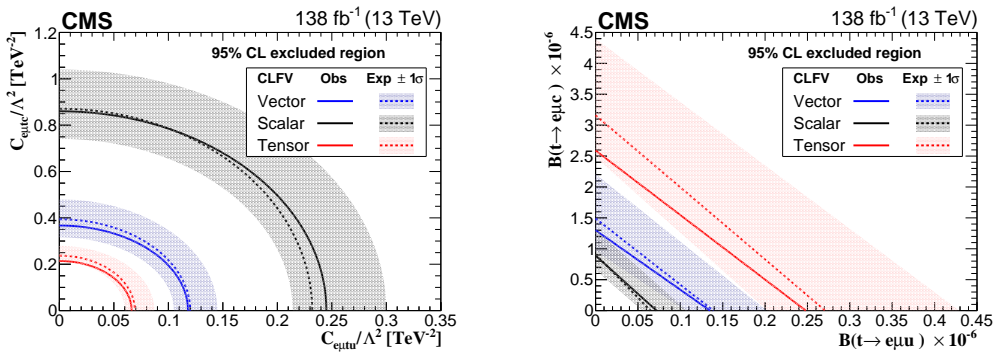

Figure 4: Observed exclusion limits at 95 % CL on the Wilson coefficients over mass scale squared (left) and the branching ratio (right) of cLFV top decays interpreted in an effective field theory approach [10].

Observed upper limits at 90 % CL			
$\mathscr{B}(B^0 \to K^{*0}e^\pm\mu^\mp)$	$< 10.1 \times 10^{-9}$	$\mathscr{B}(B_s^0 \to \phi e^\pm\mu^\mp)$	$< 16.0 \times 10^{-9}$
$\mathscr{B}(B^0 \to K^{*0}e^-\mu^+)$	$< 5.7 \times 10^{-9}$	$\mathscr{B}(B^0 \to K^{*0}\mu^-\tau^+)$	$< 1.0 \times 10^{-5}$
$\mathscr{B}(B^0 \to K^{*0}e^+\mu^-)$	$< 6.8 \times 10^{-9}$	$\mathscr{B}(B^0 \to K^{*0}\mu^+\tau^-)$	$< 8.2 \times 10^{-6}$

Table 2: Observed upper limits at 90 % CL on $B^0 \to K^{*0}\ell\ell'$ and $B_s^0 \to \phi e^\pm\mu^\mp$ decays [12, 13].

in an effective field theory approach with vector, scalar or tensor interactions. Exclusion limits at 95 % CL for the effective couplings and branching ratios are shown in Fig. 4.

The LHC has started Run 3 of operation in 2022. ATLAS and CMS envisage to collect 300 fb^{-1} of pp collision data in Run 3, thus more than doubling the current data set. With the High Luminosity LHC upgrade, another factor of ten more data will be collected with a total expected integrated luminosity of around 3000 fb^{-1}. The gain in statistics as well as the improvement of the detectors, triggers and analysis techniques will allow to expand the sensitivity of cLFV searches at the LHC.

3. *B*-physics experiments

LFV processes can occur as well in decays of *B* mesons which are typically studied in *B*-physics experiments such as the BaBar, Belle, CLEO and LHCb experiments. Exclusion limits for LFV *B* decays range from 10^{-4} to 10^{-9} depending of the number of observed *B* decays and the background contributions present in the channel under study. An overview is provided by the Heavy Flavor Averaging Group (HFLAV) [11]. Here, recent LHCb results are presented exemplary.

LHCb has conducted a search for $B^0 \to K^{*0}e^\pm\mu^\mp$ and $B_s^0 \to \phi e^\pm\mu^\mp$ [12], as well as for $B^0 \to K^{*0}\mu^\pm\tau^\mp$ [13] with the Run 1 and Run 2 data set of 9 fb^{-1} of pp collisions collected at $\sqrt{s}$ of and 7, 8 and 13 TeV. K^{*0} mesons are reconstructed by the decay to $K^+\pi^-$, ϕ mesons by the decay to an K^+K^- pair, and τ leptons by the hadronic decay mode into at least three charged pions $\pi^-\pi^+\pi^-(\pi^0)\nu_\tau$. As normalisation modes, the decays $B^0 \to J/\psi K^{*0}$ and $B_s^0 \to J/\psi\phi$ with the J/ψ resonance decaying to a $\mu^+\mu^-$ pair, as well $B^0 \to D^-D_s^+$ with $D^- \to K^+\pi^-\pi^-$ and $D_s^+ \to K^+K^-\pi^+$ are deployed. In the case of the $e\mu$ channel, the search is performed on the invariant mass spectrum of the $K\pi e\mu$ or $KKe\mu$ system, respectively. Due to the neutrino in the final state, the corrected mass is used in the case of the $\mu\tau$ channel (see Fig. 5).

With no statistically significant excess found, exclusion limits are set in the order of 10^{-9} in the $e\mu$ channel and 10^{-5} in the $\mu\tau$ channel (see Table 2).

Another LHCb search on the Run 1 and Run 2 data set concerns the decay of B^0 and B_s^0 mesons to $p\mu^-$ [14] which violates not only lepton flavour but also baryon and lepton number conservation. In this search, the decays $B^0 \to K^+\pi^-$ as well as $B^+ \to J/\psi K^+$ with subsequent $J/\psi \to \mu^+\mu^-$ decay are used as normalisation modes. As shown in Fig. 6, no statistically significant excess is observed in the invariant mass spectra of the $p\mu^-$ system. Exclusion limits are set at $\mathscr{B}(B^0 \to p\mu^-) < 2.6 \times 10^{-9}$ and $\mathscr{B}(B_s^0 \to p\mu^-) < 12.1 \times 10^{-9}$ at 90 % CL.

Furthermore, a large number of τ leptons are produced at *B*-physics and collider experiments which allow for a variety of cLFV searches in τ decays. Current exclusion limits stem from the
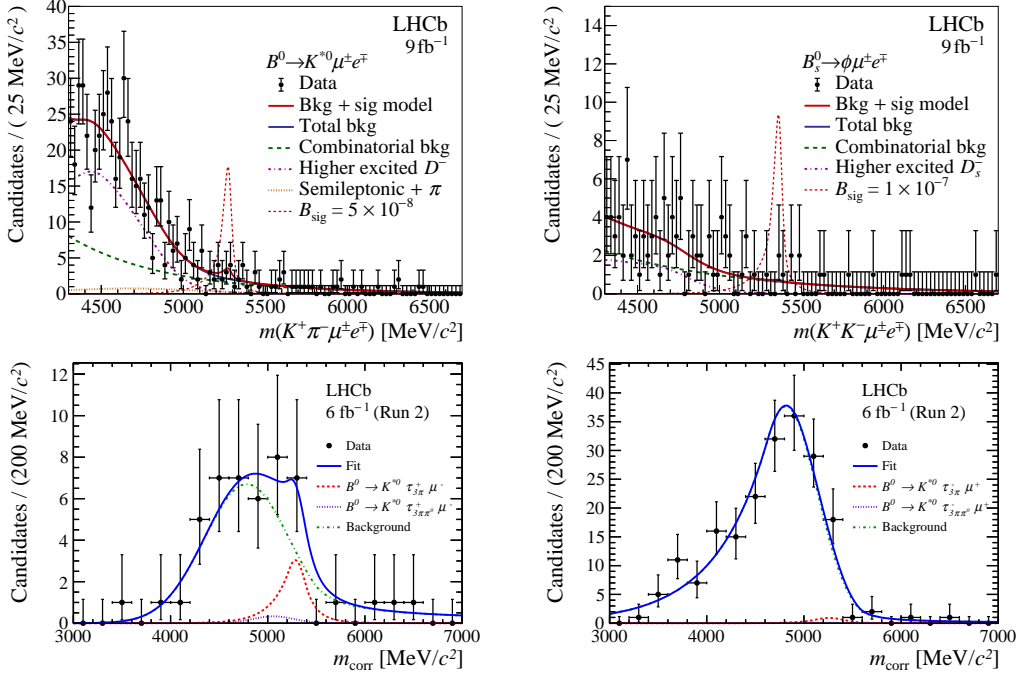
Figure 5: Observed distributions of the invariant and corrected mass, respectively, in the search for cLFV $B^0 \to K^{*0}e^{\pm}\mu^{\mp}$ (top left), $B^0_s \to \phi e^{\pm}\mu^{\mp}$ (top right), $B^0 \to K^{*0}\mu^-\tau^+$ (bottom left) and $B^0 \to K^{*0}\mu^+\tau^-$ (bottom right) decays [12, 13].
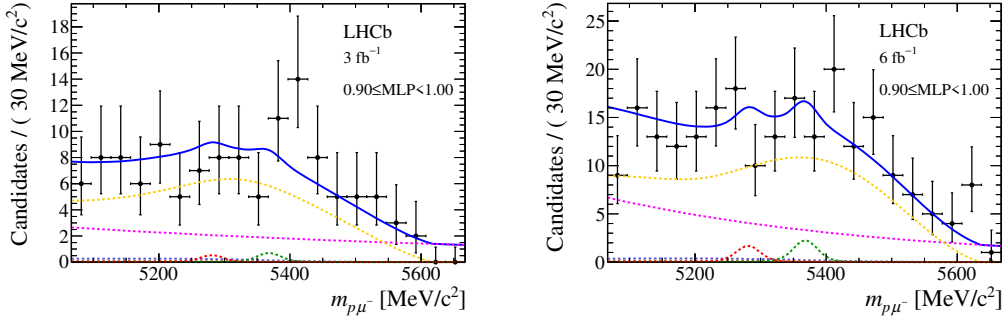

Figure 6: Observed distribution of the invariant mass in the search for cLFV $B^0_{(s)} \to p\mu^-$ decays [14].

BaBar, Belle, CLEO and LHCb as well as the ATLAS and CMS experiments and range from 10^{-6} to 10^{-8} with prospects to reach sensitivities in the range of 10^{-9} to 10^{-10} at the Belle II experiment. A summary of cLFV τ decay searches is provided by HFLAV [15]. As examples, $\tau \to \ell\gamma$ and $\tau \to \ell\ell\ell$ searches are presented in the following.

The BaBar experiment has performed a search for $\tau^{\pm} \to e^{\pm}\gamma$ and $\tau^{\pm} \to \mu^{\pm}\gamma$ in a data set of almost 10^9 τ decays from e^+e^- annihilation data collected near the $\Upsilon(4S)$, $\Upsilon(3S)$ and $\Upsilon(2S)$ resonance [16]. The distributions of events in the beam energy constrained τ mass m_{EC} of the $\ell\gamma$ pair and in the energy difference $\Delta E = E_{\ell\gamma}^{CM} - \frac{\sqrt{s}}{2}$ of the total energy in the centre-of-mass frame and the beam energy after selections are shown in Fig. 7. In the absence of an evidence for a signal,
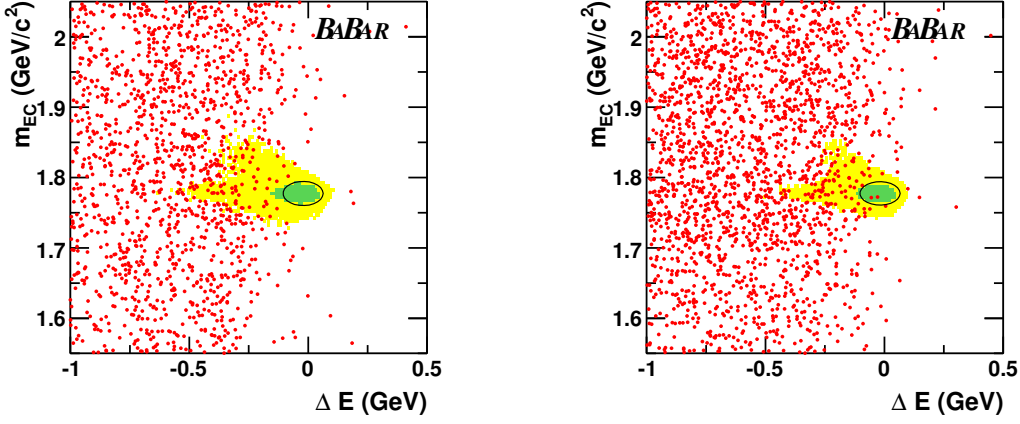
Figure 7: Distribution of observed events in the ΔE vs. m_{EC} plane in the $\tau^{\pm} \to e^{\pm}\gamma$ (left) and $\tau^{\pm} \to \mu^{\pm}\gamma$ (right) search [16]. The signal region is indicated by an ellipse. The region containing 90 % (50 %) of simulated signal events is indicated in yellow (green).

Observed upper limits at 90 % CL			
$\mathscr{B}(\tau^- \to e^- e^+ e^-)$	$< 2.7 \times 10^{-8}$	$\mathscr{B}(\tau^- \to \mu^- \mu^+ \mu^-)$	$< 2.1 \times 10^{-8}$
$\mathscr{B}(\tau^- \to e^- \mu^+ \mu^-)$	$< 2.7 \times 10^{-8}$	$\mathscr{B}(\tau^- \to \mu^- e^+ e^-)$	$< 1.8 \times 10^{-8}$
$\mathscr{B}(\tau^- \to e^+ \mu^- \mu^-)$	$< 1.7 \times 10^{-8}$	$\mathscr{B}(\tau^- \to \mu^+ e^- e^-)$	$< 1.5 \times 10^{-8}$

Table 3: Observed upper limits at 90 % CL on cLFV $\tau \to \ell\ell\ell$ decays [17].

upper limits are set at $\mathscr{B}(\tau^{\pm} \to e^{\pm}\gamma) < 3.3 \times 10^{-8}$ and $\mathscr{B}(\tau^{\pm} \to \mu^{\pm}\gamma) < 4.4 \times 10^{-8}$ at 90 % CL.

At the Belle experiment, a search for $\tau^- \to \ell^- \ell^+ \ell^-$ has been conducted for all possible combinations of e and μ in the final state with a data set of 782 fb^{-1} of e^+e^- annihilation data collected near the $\Upsilon(4S)$ resonance [17]. As shown in Fig. 8, no event is observed in the signal region of the search. The derived exclusion limits are summarised in Table 3.

4. Kaon decays

Kaons and pions are produced in large quantities at fixed-target experiments such as the experiments E865 and E871 at the Alternating Gradient Synchrotron at Brookhaven National Laboratory (BNL), the KTeV experiment at the Tevatron at Fermilab, and NA62 at the Super Proton Synchrotron (SPS) at CERN. Searches are conducted for LFV pion and kaon decays as well as lepton flavour and lepton number violating kaon decays. Current exclusion limits range from 10^{-10} down to 10^{-12}. A summary is given in Table 4.

As an example, a search for the decays $K^+ \to \pi^- e^+ \mu^+$, $K^+ \to \pi^+ e^+ \mu^-$ and $\pi^0 \to e^+ \mu^-$ by the NA62 experiment is presented in the following [18]. The data set has been collected from 8.3×10^5 spills of the SPS in 2017 and 2018. The decay $K^+ \to \pi^+ \pi^+ \pi^-$ is used as normalisation mode. The $\pi^0 \to e^+ \mu^-$ search is performed on a subset of events from the $K^+ \to \pi^+ e^+ \mu^-$ search. In this case, the π^0 stems from a $K^+ \to \pi^+ \pi^0$ decay and the invariant mass of the $e^+ \mu^-$ pair is required to be

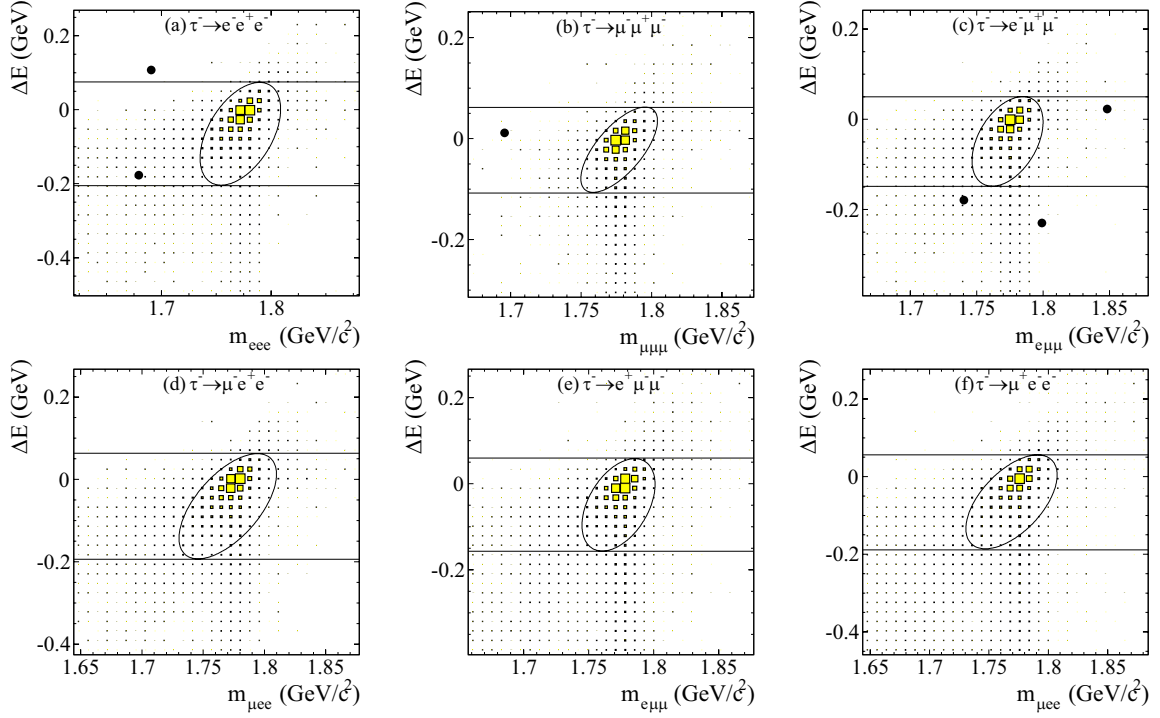**Figure 8:** Distribution of observed events (black dots) in the invariant mass vs. ΔE plane in the search for cLFV $\tau \to \ell\ell\ell$ decays [17]. The distribution of simulated signal events is indicated by yellow boxes and the signal region by ellipses.

consistent with the π^0 mass. No excess has been found in the invariant mass spectra of the $\pi e \mu$ system (see Fig. 9). The corresponding exclusion limits are listed in Table 4.

5. Muon decays

The three golden channels of muon cLFV searches, $\mu \to e\gamma$, $\mu \to eee$ and muon-to-electron conversion on nuclei are subject of a global experimental initiative that will push the sensitivity to muon cLFV processes by several orders of magnitude in the coming years.

The first experiment of this kind is the MEG experiment searching for $\mu^+ \to e^+\gamma$ which operated from 2009 to 2013 at the Paul Scherrer Institute (PSI) [23], and its upgrade MEG II which is taking physics data since 2021 [24].

The MEG experiment is optimised for the back-to-back signature of $\mu^+ \to e^+\gamma$ decays from μ^+ stopped on the target in the centre of the detector. The photon is measured with a liquid Xenon calorimeter, and the positron with a combination of a drift chamber array and scintillating timing counters placed in the COnstant Bending RAdius magnet (see Fig. 10a). Background from radiative muon decays $\mu^+ \to e^+\gamma\nu\bar{\nu}$ as well as from accidental coincidences of positrons and photons from different sources is suppressed by selections on the positron and photon energies E_e and E_γ, the relative stereo angle $\Theta_{e\gamma}$ and the relative time $t_{e\gamma}$. The experiment is operated at a continuous μ^+ beam to lower background contributions from accidental coincidences.

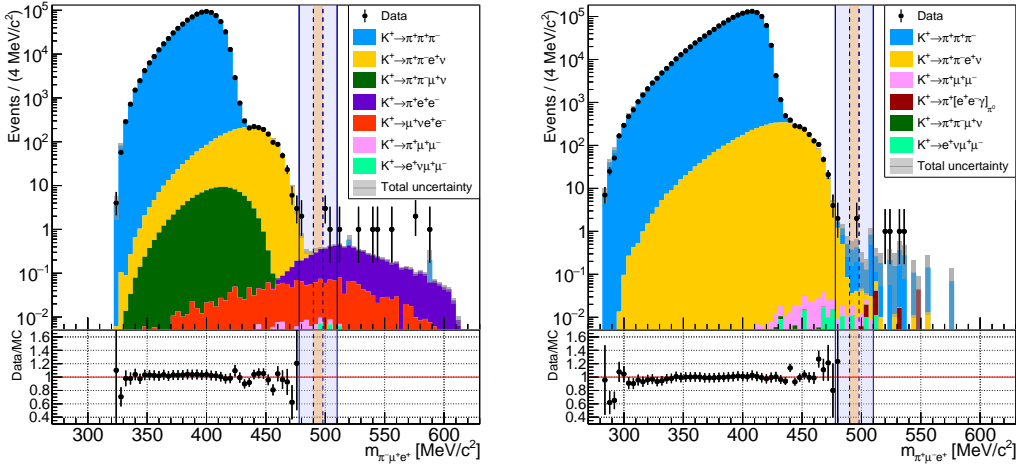| Observed upper limits at 90 % CL		Experiment
$\mathscr{B}(K^+ \to \pi^- e^+ \mu^+)$	$< 4.2 \times 10^{-11}$	NA62 at CERN [18]
$\mathscr{B}(K^+ \to \pi^+ e^+ \mu^-)$	$< 6.6 \times 10^{-11}$	NA62 at CERN [18]
$\mathscr{B}(K^+ \to \pi^+ e^- \mu^+)$	$< 1.3 \times 10^{-11}$	E865 at BNL [19]
$\mathscr{B}(K_L^0 \to e^\pm \mu^\mp)$	$< 4.7 \times 10^{-12}$	E871 at BNL [20]
$\mathscr{B}(K_L^0 \to \pi^0 e^\pm \mu^\mp)$	$< 7.6 \times 10^{-11}$	KTeV at Fermilab [21]
$\mathscr{B}(K_L^0 \to \pi^0 \pi^0 e^\pm \mu^\mp)$	$< 1.7 \times 10^{-10}$	KTeV at Fermilab [21]
$\mathscr{B}(\pi^0 \to e^+ \mu^-)$	$< 3.2 \times 10^{-10}$	NA62 at CERN [18]
$\mathscr{B}(\pi^0 \to e^- \mu^+)$	$< 3.8 \times 10^{-10}$	E865 at BNL [22]
$\mathscr{B}(\pi^0 \to e^\pm \mu^\mp)$	$< 3.6 \times 10^{-10}$	KTeV at Fermilab [21]

Table 4: Observed upper limits at 90 % CL on cLFV kaon decays.

Figure 9: Observed distributions of the invariant mass in the search for $K^+ \to \pi^- e^+ \mu^+$ (left) and $K^+ \to \pi^+ e^+ \mu^-$ (right) [18].

MEG has recorded 7.5×10^{14} μ^+ decays. The distribution of the observed events in the respective observables is shown in Fig. 11. With no significant excess observed with respect to the expected background, an upper limit on the $\mu^+ \to e^+ \gamma$ decay is set at $\mathscr{B} < 4.2 \times 10^{-13}$ at 90 % CL.

MEG II poses a substantial upgrade of the MEG experiment which significantly increased the rate capability and detector resolution (see Fig. 10b). For MEG II, a sensitivity to branching ratios down to 6×10^{-14} at 90 % CL is expected allowing to push the limit of MEG by another order of magnitude [24].

In the case of a $\mu^+ \to e^+ e^- e^+$ search, background stems from the rare decay $\mu^+ \to e^+ e^- e^+ \nu \bar{\nu}$ as well as accidental coincidences of e^+ and e^- which can be suppressed by selections on the relative timing as well as kinematic observables of the $e^+ e^- e^+$ system such as the invariant mass m_{eee}. Such searches are conducted with a continuous μ^+ beam. The latest search has been performed by the SINDRUM experiment [25] at PSI. As no signal decay has been observed, an upper limit is set on the branching ratio at $\mathscr{B} < 1.0 \times 10^{-12}$ at 90 % CL.
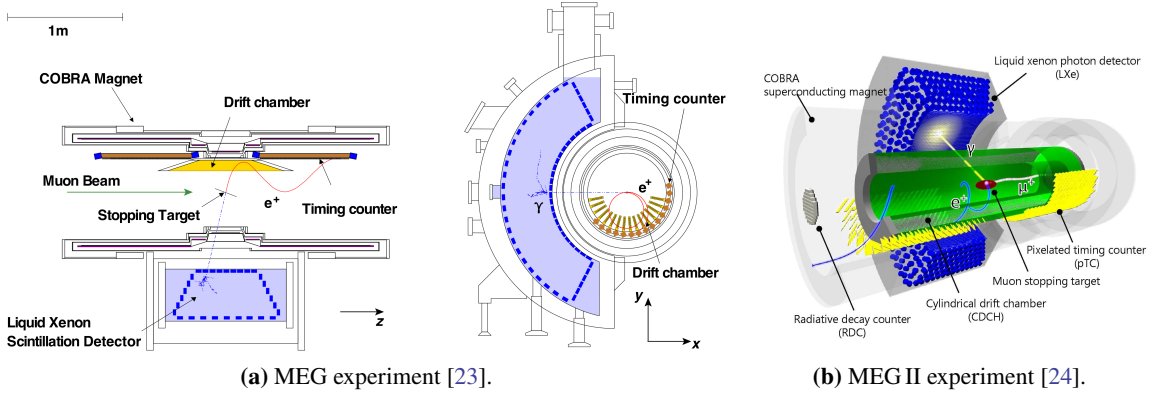
(a) MEG experiment [23].   **(b)** MEG II experiment [24].

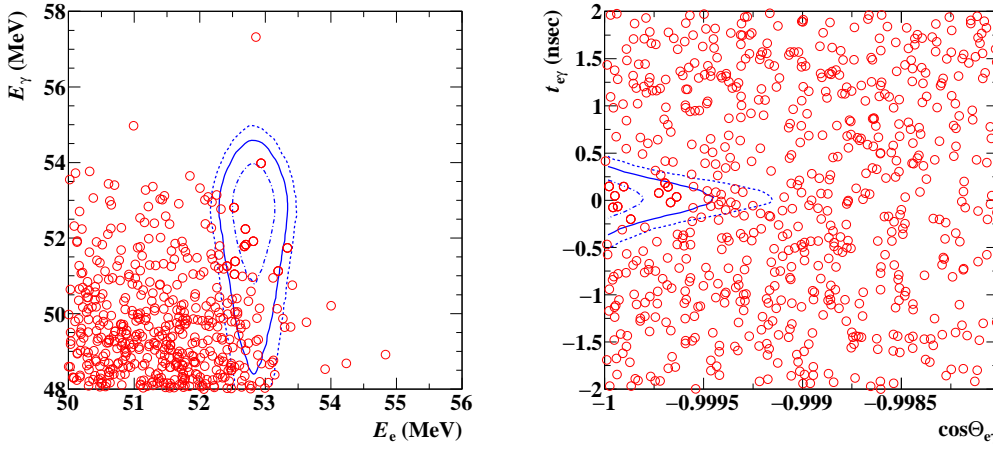**Figure 10:** Sketches of the MEG and MEG II experiments [23, 24].

Figure 11: Distribution of observed events (red circles) in the E_e vs. E_γ (left) and $\Theta_{e\gamma}$ vs. $t_{e\gamma}$ plane in the $\mu^+ \to e^+\gamma$ search [23]. Blue lines indicate the 1σ, 1.64σ and 2σ contours of the signal probability density function, respectively.

The upcoming Mu3e experiment at PSI is going to repeat the search [26]. The detector design is optimised to mitigate the deteriorating effects of multiple scattering on the momentum measurement of e^+ and e^- by having a large lever arm between single measurement points and by reducing the amount of material in the active detector volume to a minimum (see Fig. 12). In order to cope with the expected high event rate, the experiment deploys real-time event reconstruction and filtering instead of a hardware trigger. In a first phase, the experiment will be operated at an existing beam line with a muon stopping rate of around $10^8\,\mu$/s yielding an expected sensitivity to branching ratios of about 10^{-15} (see Fig. 13). In the second phase, an upgraded detector will be operated at a new beam line at PSI – the High Intensity Muon Beams [27] – at stopping rates around $2 \times 10^9\,\mu$/s reaching the final sensitivity to branching ratios of about 10^{-16}.

LFV processes can also occur in muonic atoms in the muon-to-electron conversion process $\mu^- N \to e^- N$ on a nucleus N. The characteristic signature of this conversion is a mono-energetic e^-. In addition to muon decay in orbit of the muonic atom and radiative muon capture, there are beam related backgrounds from muon decays in flight and contamination from pions and electrons, as well
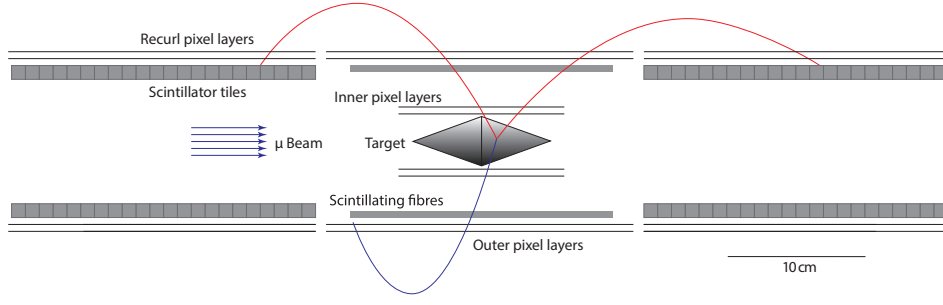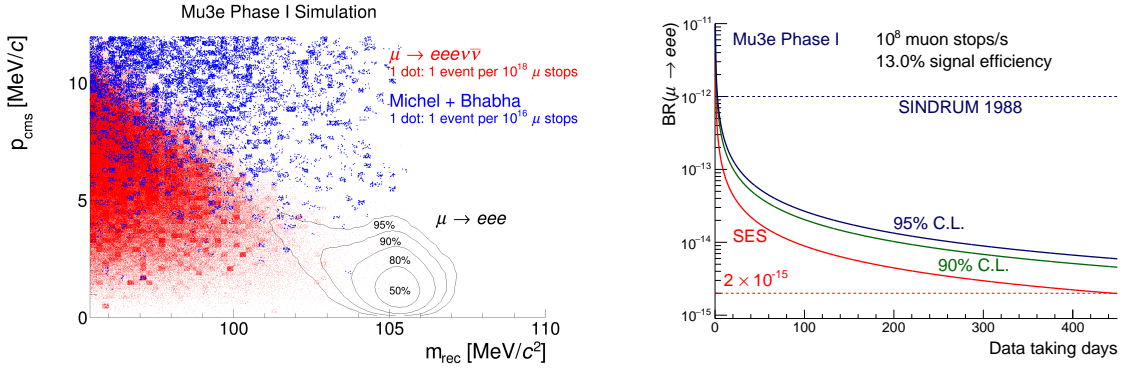
Figure 12: Sketch of the Mu3e phase I experiment [26].

(a) Distribution of simulated background events and signal contour in the invariant mass vs. centre-of-mass momentum plane.

(b) Expected sensitivity to $\mathscr{B}(\mu \to eee)$ with respect to the data taking period.

Figure 13: Sensitivity of the Mu3e phase I experiment [26].

as background from cosmics. Beam related backgrounds are reduced by using a pulsed μ^- beam and starting data recording only several 100 ns after the pulse when the majority of contamination has already decayed. Further reduction is achieved by separating the production target from the muon stopping target.

The current most stringent limit on the conversion rate has been set by the SINDRUM II experiment at $R_{\mu e}(\mu^-\text{Au} \to e^-\text{Au}) < 7.0 \times 10^{-13}$ [28]. Three experiments will repeat this search in the near future.

The DeeMe experiment at J-Parc is currently being commissioned [29]. In DeeMe, the production and stopping target are combined. Electrons from background processes are filtered out in a secondary beam line and the remaining electrons are measured in a magnetic spectrometer. The expected single-event sensitivity for $R_{\mu e}(\mu^-\text{C} \to e^-\text{C})$ lies at 1×10^{-13}.

The COherent Muon to Electron Transition experiment at J-Parc is currently under construction [30]. In the phase I experiment, the production and stopping target are separated by a $90°$ muon transport solenoid (see Fig. 14a). The stopping target is located within the detector section. Operating at a stopping rate of around $1.2 \times 10^9\,\mu/\text{s}$, the experiment has an expected sensitivity to $R_{\mu e}(\mu^-\text{Al} \to e^-\text{Al})$ as small as 7×10^{-15} at 90% CL. In phase II, stopping target and detector section are separated by a C-shaped electron spectrometer (see Fig. 14b). In addition, the muon transport section is extended from a $90°$ to a full $180°$ turn. Combined with an increased proton beam
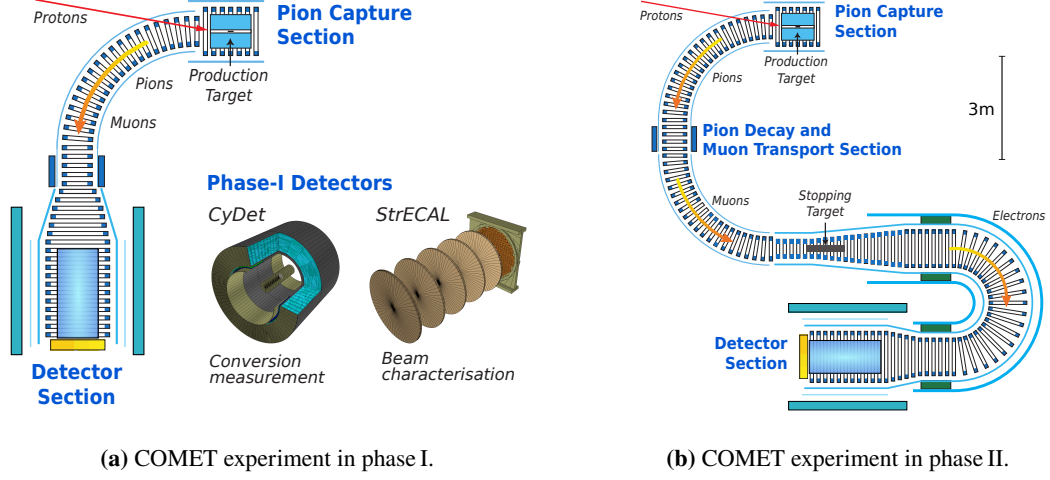
11

(a) COMET experiment in phase I.   **(b)** COMET experiment in phase II.

Figure 14: Sketch of the COMET experiment in phase I and phase II [30].

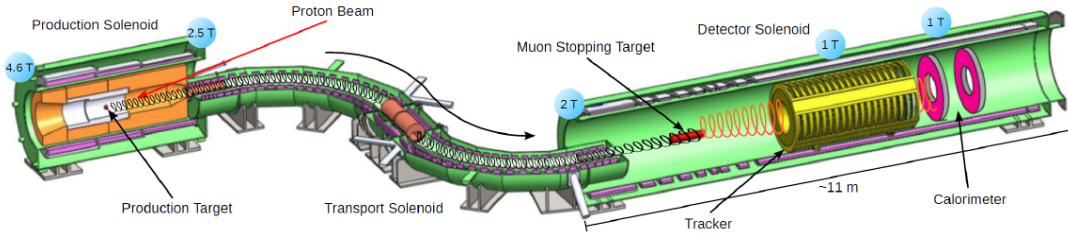**Figure 15:** Sketch of the Mu2e experiment [31].

intensity and an upgraded production target, conversion rates of $R_{\mu e}(\mu^- \mathrm{Al} \to e^- \mathrm{Al}) \geq 2.6 \times 10^{-17}$ at 90 % CL are in reach of COMET phase II.

At Fermilab, the Mu2e experiment is currently being constructed [31]. Here, production and stopping target are separated by a transport solenoid (see Fig. 15). The muon stopping target is located in front of the straw tube tracker and the calorimeter inside the detector solenoid. The experiment is operated at muon stopping rates of around $10^{10}\ \mu/\mathrm{s}$. In the first run, Mu2e is expected to be sensitive to $R_{\mu e}(\mu^- \mathrm{Al} \to e^- \mathrm{Al})$ down to 6.6×10^{-16} at 90 % CL. Continuing data taking after the long shutdown at Fermilab, the experiment will reach its goal sensitivity to $R_{\mu e}(\mu^- \mathrm{Al} \to e^- \mathrm{Al})$ of 6×10^{-17} at 90 % CL.

In addition to the three golden channels, cLFV decays of the type $\mu \to eX$ and $\mu \to e\gamma X$ can be studied. The X particle can either decay – to $e^+ e^-$, $\nu\bar{\nu}$ or $\gamma\gamma$ – or be stable or long-lived such that it remains invisible in experiments. The current most stringent limits for $\mu \to e\gamma X$ with X lighter than twice the electron mass are set by the Crystal Box experiment at $\mathscr{B}(\mu^+ \to e^+ \gamma X) < 1.1 \times 10^{-9}$ at 90 % CL [32]. For massless X in $\mu \to eX$, an upper exclusion limit has been set at $\mathscr{B}(\mu^+ \to e^+ X) < 2.6 \times 10^{-6}$ at 90 % CL by Jodidio et al. [33]. The TWIST experiment has derived upper exclusion limits of $\mathscr{B}(\mu^+ \to e^+ X) < 9 \times 10^{-6}$ at 90 % CL on average for X with masses between 13 MeV and 80 MeV [34] (see Fig. 16a).

(a) Upper exclusion limits on $\mathscr{B}(\mu^+ \to e^+ X)$ at 90 % CL set by the TWIST experiment [34].

(b) Prospected sensitivity of the Mu3e phase I experiment to $\mathscr{B}(\mu^+ \to e^+ X)$ at 90 % CL [35].

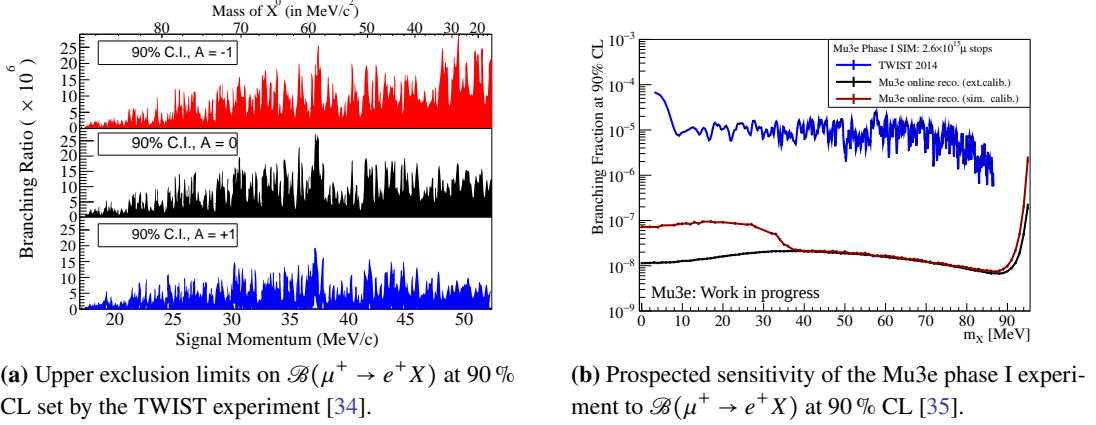**Figure 16:** Current most stringent upper limits on and prospected sensitivity to $\mathscr{B}(\mu^+ \to e^+ X)$.

Currently, there are discussions at the MEG II, Mu3e, COMET and Mu2e experiments to conduct $\mu \to eX$ or $\mu \to e\gamma X$ searches as well. Given the large number of muon decays to be investigated at these experiments, improvements in the sensitivity of two to three orders of magnitude compared to current limits are expected. As an example, the prospected sensitivity of the Mu3e phase I experiment to $\mu^+ \to e^+ X$ decays is shown in Fig. 16b.

6. Conclusion

The observation of cLFV processes would be an unambiguous sign of BSM physics. Searches are conducted in various channels at general-purpose experiments, at *B*- and kaon-physics experiments and at dedicated LFV muon-decay experiments. So far, no cLFV processes have been observed. Several experiments are currently in operation or will soon commence data taking. Thus, ever smaller branching ratios can be investigated. In some cases, the sensitivity is pushed by three to four orders of magnitude. This allows to probe models predicting cLFV with high precision or potentially discover BSM physics.

References

[1] L. Calibbi and G. Signorelli, *Charged lepton flavour violation: An experimental and theoretical introduction*, *Riv. Nuovo Cim.* **41** (2018) 71 [1709.00294].

[2] CMS collaboration, *Search for heavy resonances and quantum black holes in eμ, eτ, and μτ final states in proton-proton collisions at $\sqrt{s}$ = 13 TeV*, 2205.06709.

[3] ATLAS collaboration, *Search for the Higgs boson decays H → ee and H → eμ in pp collisions at $\sqrt{s}$ = 13 TeV with the ATLAS detector*, *Phys. Lett. B* **801** (2020) 135148 [1909.10235].

[4] ATLAS collaboration, *Search for the charged-lepton-flavor-violating decay Z → eμ in pp collisions at $\sqrt{s}$ = 13 TeV with the ATLAS detector*, 2204.10783.

[5] CMS collaboration, *Search for the lepton flavor violating decay of a Higgs boson in the eμ final state in proton-proton collisions at $\sqrt{s}$ = 13 TeV*, CMS-PAS-HIG-22-002 (2023) .

[6] CMS collaboration, *Search for lepton-flavor violating decays of the Higgs boson in the μτ and eτ final states in proton-proton collisions at $\sqrt{s}$ = 13 TeV*, *Phys. Rev. D* **104** (2021) 032013 [2105.03007].

[7] ATLAS collaboration, *Searches for lepton-flavour-violating decays of the Higgs boson into eτ and μτ in $\sqrt{s}$ = 13 TeV pp collisions with the ATLAS detector*, 2302.05225.

[8] ATLAS collaboration, *Search for charged-lepton-flavour violation in Z-boson decays with the ATLAS detector*, *Nature Phys.* **17** (2021) 819 [2010.02566].

[9] ATLAS collaboration, *Search for lepton-flavor-violation in Z-boson decays with τ-leptons with the ATLAS detector*, *Phys. Rev. Lett.* **127** (2022) 271801 [2105.12491].

[10] CMS collaboration, *Search for charged-lepton flavor violation in top quark production and decay in pp collisions at $\sqrt{s}$ = 13 TeV*, *JHEP* **06** (2022) 082 [2201.07859].

[11] HFLAV collaboration, *Averages of b-hadron, c-hadron, and τ-lepton properties as of 2021*, 2206.07501.

[12] LHCʙ collaboration, *Search for the lepton-flavour violating decays $B^0 \to K^{*0}\mu^\pm e^\mp$ and $B_s^0 \to \phi\mu^\pm e^\mp$*, 2207.04005.

[13] LHCʙ collaboration, *Search for the lepton-flavour violating decays $B^0 \to K^{*0}\tau^\pm\mu^\mp$*, 2209.09846.

[14] LHCʙ collaboration, *Search for the baryon- and lepton-number violating decays $B^0 \to p\mu^-$ and $B_s^0 \to p\mu^-$*, 2210.10412.

[15] HFLAV collaboration, *Averages of b-hadron, c-hadron, and τ-lepton properties as of 2018*, *Eur. Phys. J. C* **81** (2021) 226 [1909.12524].

[16] BaBar collaboration, *Searches for lepton flavor violation in the decays $\tau^\pm \to e^\pm\gamma$ and $\tau^\pm \to \mu^\pm\gamma$*, *Phys. Rev. Lett.* **104** (2010) 021802 [0908.2381].

[17] Belle collaboration, *Search for lepton flavor violating τ decays into three leptons with 719 million produced $\tau^+\tau^-$ pairs*, *Phys. Lett. B* **687** (2010) 139 [1001.3221].

[18] NA62 collaboration, *Search for lepton number and flavor violation in K^+ and π^0 decays*, *Phys. Rev. Lett.* **127** (2021) 131802 [2105.06759].

[19] A. Sher, R. Appel, G.S. Atoyan, B. Bassalleck, D.R. Bergman, N. Cheung et al., *Improved upper limit on the decay $K^+ \to \pi^+\mu^+e^-$*, *Phys. Rev. D* **72** (2005) 012005 [hep-ex/0502020].

[20] BNL E871 collaboration, *New limit on muon and electron lepton number violation from $K_L^0 \to \mu^\pm e^\mp$ decay*, *Phys. Rev. Lett.* **81** (1998) 5734 [hep-ex/9811038].

[21] KTeV collaboration, *Search for lepton flavor violating decays of the neutral kaon*, *Phys. Rev. Lett.* **100** (2008) 131803 [0711.3472].

[22] R. Appel, G.S. Atoyan, B. Bassalleck, D.R. Bergman, D.N. Brown, N. Cheung et al., *Improved limit on the rate of the decay $K^+ \to \pi^+ \mu^+ e^-$*, *Phys. Rev. Lett.* **85** (2000) 2450 [hep-ex/0005016].

[23] MEG collaboration, *Search for the lepton flavour violating decay $\mu^+ \to e^+ \gamma$ with the full dataset of the MEG experiment*, *Eur. Phys. J. C* **76** (2016) 434 [1605.05081].

[24] MEG II collaboration, *The design of the MEG II experiment*, *Eur. Phys. J. C* **78** (2018) 380 [1801.04688].

[25] SINDRUM collaboration, *Search for the decay $\mu^+ \to e^+ e^+ e^-$*, *Nucl. Phys. B* **299** (1988) 1.

[26] Mu3e collaboration, *Technical design of the phase I Mu3e experiment*, *Nucl. Instrum. Meth. A* **1014** (2021) 165679 [2009.11690].

[27] M. Aiba et al., *Science case for the new High-Intensity Muon Beams HIMB at PSI*, 2111.05788.

[28] SINDRUM II collaboration, *A Search for muon to electron conversion in muonic gold*, *Eur. Phys. J. C* **47** (2006) 337.

[29] DeeMe collaboration, *DeeMe experiment - An experimental search for a mu-e conversion reaction at J-PARC MLF*, *Nucl. Phys. B Proc. Suppl.* **248-250** (2014) 52.

[30] COMET collaboration, *COMET phase-I technical design report*, *PTEP* **2020** (2020) 033C01 [1812.09018].

[31] Mu2e collaboration, *Mu2e technical design report*, 1501.05241.

[32] R.D. Bolton et al., *Search for rare muon decays with the Crystal Box detector*, *Phys. Rev. D* **38** (1988) 2077.

[33] A. Jodidio et al., *Search for right-handed currents in muon decay*, *Phys. Rev. D* **34** (1986) 1967.

[34] TWIST collaboration, *Search for two body muon decay signals*, *Phys. Rev. D* **91** (2015) 052020 [1409.0638].

[35] Mu3e collaboration, *The rare and forbidden: Testing physics beyond the standard model with Mu3e*, *SciPost Phys. Proc.* **1** (2019) 052 [1812.00741].

Acknowledgments